International Journal of Current Science, Engineering & Technology ISSN : 2581-4311
Original Research Article | Open Access | AMCT 2017 Malaysia | *Special Issue*

Improved Performance of Dye Sensitized Solar Cell with Nb-Doped TiO_2 Photoanodes using Solid State Method

Hidayani JAAFAR[1,a,c*], Zainal Arifin AHMAD[2,a] and Mohd Fadzil AIN[3,b]

[1]Structural Materials Niche Area, School of Materials and Minerals Resources Engineering, UniversitiSains Malaysia, Engineering Campus, 14300 NibongTebal, Penang, Malaysia.

[2]School of Electrical and Electronic Engineeering, UniversitiSains Malaysia, Engineering Campus, 14300 NibongTebal, Penang, Malaysia.

[3]Faculty of Bioengineering and Technology, Universiti Malaysia Kelantan, 17600 Jeli, Kelantan, Malaysia.

[a]hidayani@umk.edu.my, [b]srzainal@usm.my, [c]eemfadzil@usm.my

ABSTRACT. A series ofNb-doped TiO_2 (0.25-1.75 wt.% of Nb) were synthesized via solid state technique and used for the development of photoanodes in dye-sensitized solar cells (DSSCs). The X-ray diffraction patterns of the Nb-doped TiO_2 were almost exactly matched to pure anatase TiO_2 with no Nb_2O_5 peaks observed. It was found that, 1.0 wt.% Nb had the highest energy conversion efficiency (η) of 1.40%, short current density (J_{SC}) of 5.00 mA/cm^2 and open circuit voltage (V_{OC}) of 0.33V. From electrochemical impedance (EIS) measurements, the presence of Nb dopants has enhanced the cell performance by improving the charge transport and retarding the recombination process in the photoanode.

Keywords: *Nb-doped TiO_2, Photoanode, Dye sensitized solar cell;*

Received: 15.10.2017, Revised: 15.12.2017, Accepted: 30.02.2018, and Online: 20.03.2018;

DOI: ***10.30967/ijcrset.1.S1.2018.256-261***

Selection and/or Peer-review under responsibility of Advanced Materials Characterization Techniques (AMCT 2017), Malaysia.

1. INTRODUCTION

Dye-sensitized solar cells (DSSCs) have received great attention due to the low cost and easy fabrication process as well as its high power conversion efficiency [1]. A typical DSSC consists of multiple components i.e. transpiring conducting glass which usually utilizes fluorine-doped tin oxide (FTO) or indium-doped tin oxide (ITO), mesoporous metal oxide layer developed from TiO_2 that acts as photoanode, sensitizers (dye molecules), electrolyte (iodide-tri iodide electrolyte is mostly used) and counter electrode. TiO_2 (anatase) has been widely used as photoanode to ensure the transfer of photo-excited electrons. Due to its outstanding optical and electrical properties, TiO_2 has been extensively investigated as one of the most promising wide band gap semiconducting materials in photocatalysisand photovoltaic applications [2]. As a result, single-crystal TiO_2 is preferred as it can provide direct electrical pathways for photo-generated charges and avoid electron scattering or trapping [3]. When electron transport is oriented, the DSSCs can enhance performance in photoelectric conversion

Modification of photoanode in previous studies using TiO_2 based photoanodes has shown that doping with various metals could enhance some of the photovoltaic properties of the cell. Xiang et al. [4] reported the negative shifting of TiO_2 conduction band (CB) as a result of tantalum (Ta) doping; this was due to an increase in open circuit voltage (Voc) which increased the energy conversion efficiency. Kim et al. [5] reported improvements in photoelectric performance of DSSCs using chromium (Cr)-doped TiO_2 semiconductor as

photoanode. Lu et al. [6] and Nikolay et al. [7] synthesized niobium (Nb)-doped TiO_2 using the co-hydrolysis method and found an improvementin electron injection and transport due to the increase in electrical conductivity, shift of E_F and conduction band minimum (CBM).

However, it is difficult to obtain high crystallinity and size uniformity using the co-hydrolysis method; besides that, it also inevitably generates structural defects in TiO_2 which affects the electron injection and transportation. Doping via the co-hydrolysis method also tends to cause deep dopants energy which may not be available for electron injection and transportation. Moreover, the preparation of Nb-doped TiO_2 using the co-hydrolysis method is expensive and niobium chloride ($NbCl_5$) is unstable and not suitable for use in mass production [8]. Much research has been conducted on the photovoltaic performance of Nb-doped TiO_2 photoanode but its fabrication using the solid state method has not been reported. Fabrication using the solid state method tends to produce a homogeneous powder with high crystallinity structure and is less complicated compared to the co-hydrolysis method.

2. MATERIALS AND METHODS

2.1 Preparation of Natural Dye Sensitizers

Preparation and characterization of *E. confertaa*s sensitizers can be found in our previous work [9].

2.2 Preparation of Nb-doped TiO_2. TiO_2 doped with 0.25-1.75 wt.% of Nb were synthesized via the solid state method. The mixture was prepared using the ball mixing method. The mixture was filled into 250 ml polyethelene containers with zirconia balls with a ball to powder weight ratio of 10:1. Zirconia balls were used as a mixing media due to its high degree of hardness and to minimize contamination. The containers were placed on the ball mixing roller and mixed for 6 hours at 120 rpm and annealed at 600 °C for 6 hours.

2.3 Preparation of Photoanode and Assembly of DSSCs. FTO conductive glass with a sheet resistance of ~7Ω/cm^2 was cleaned in a detergent solution, rinsed using deionized water and ethanol and then dried. TiO_2 paste was prepared with 0.3 g of TiO_2, 0.5 ml acetic acid, 1:1 (5 ml) mixture of deionized water and ethanol and was ground for 20 min. Trition–X was added (0.5 ml) to the mixture and continued to be ground until a homogenous paste was achieved. The TiO_2 pastes were deposited onto FTO glass using the doctor blade technique. The coated films were sintered at 450 °C for 30 min. The same method was applied for the 0.25-1.75 wt.% Nb-doped TiO_2, respectively. The sintered photoanode electrodes were immersed in *E. Confertad*ye solution for 24 hours at room temperature. The sensitized electrodes were rinsed using ethanol to remove unanchored dye. The counter electrode was obtained according to methods employed in previous work [9]. A drop of redox electrolyte was cast on the surface of the sensitized photoanodes. The counter electrode was then clipped onto the top of TiO_2 working electrode with a cell active area of 6.5 cm^2, and then sealed using slurry tape.

2.4 Cell Characterization. Phase identification of the nanomaterials were studied using Bruker D8 Advance which was operated in Bragg Brentano geometry and exposed to CuKα radiation (λ = 1.540Å). The X-ray diffraction (XRD) pattern was scanned with step size of 0.02° (2θ) at a fixed counting time of 71.6 s from 10° to 90° 2θ. The resulting powder diffraction patterns were analyzed using Highscore Plus software. The photocurrent-voltage (J-V) curves of DSSCs were recorded with a computer-controlled digital source meter (Keithley 2400) under an irradiation of 100 $mWcm^{-2}$. The charge-transfer resistance of a DSSC was analyzed by electrochemical impedance spectroscopy (EIS, GamryREF 3000, USA) under a light intensity of 100 mW cm^{-2}in a frequency ranging from 0.1 Hz to 100 kHz with an AC amplitude of 10 mV.

3. *RESULTS AND DISCUSSION*

3.1 XRD Analysis. Fig. 1(a) shows the XRD patterns of the undoped TiO_2 (0 wt.% Nb) and Nb-doped TiO_2 (0.25–1.75 wt.% Nb). The peaks indicate that the complete anatase structure after doping with Nb showed no characteristic peaks of Nb_2O_5 in Nb-doped TiO_2 even at 1.75 wt.% Nb. In Fig. 1(a), the lattice distortion is

due to the defects (vacancies, interstitials and substitutions) which can cause shifts in XRD peak positions, depending on the type of strain in the crystal, such as tensile or compressive strain. This shift proves that the Nb^{5+} was successfully inserted into the crystal lattice of TiO_2. An observation of the enlarged image shown in Fig. 1(b) indicates a shift in peak positions as well as change in peak broadening. Based on the line from Fig. 1(b), the peaks start to shift when 0.25 wt.% onwards of Nb was doped into the TiO_2. This shows that the Nb doped into the TiO_2 lattice and is evident by the shift in peak position towards a higher angle. In addition, the full-width at half maximum of XRD patterns of the sample are sharpened with the increase of Nb doping concentration which might be attributed to the increased of crystallite size. By using DebyeScherrer equation, the crystallite sizes of these samples are listed in Table 1. The introduction of Nb into TiO_2 can inhibited the crystallite size. This is in line with the peak shifted as shown in Fig. 1(b). The lattice constant (*a*and *c*) and cell volume also increases when the amount of Nb increases. Therefore, there have significant changes in crystal parameters when the amount of Nb increases based on lattice constant and crystallite size analysis which affect the performance of DSSC.

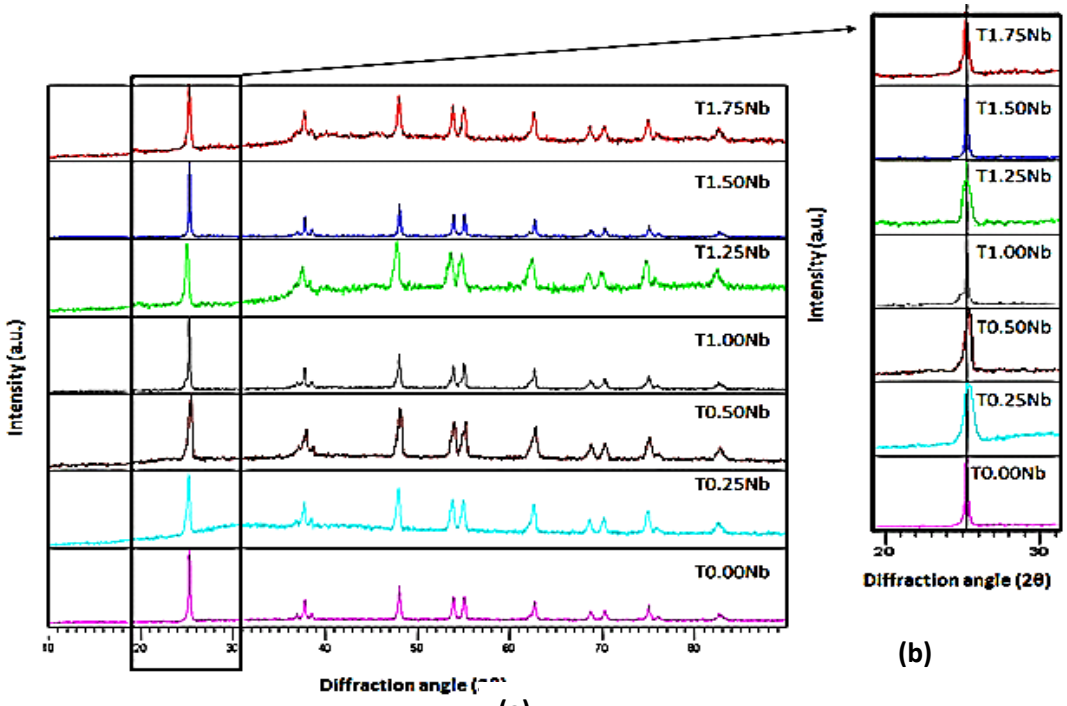

Fig. 1 (a) XRD patterns of 0-1.75 wt.% Nb-d iO2 and (b) Shifts in peak position and changes in peak broadening are depicted through enlarged view of (101) peaks for undoped TiO_2 and Nb-doped TiO_2

Table 1 Lattice parameter, average crystallite size of Nb-doped TiO_2

Sample	Average crystallite size (nm)	a (Å)	c (Å)
0 wt.% Nb	8.51	3.784	9.49
0.25 wt.% Nb	9.16	3.784	9.50
0.5 wt.% Nb	9.16	3.785	9.50
1.0 wt.% Nb	11.00	3.785	9.50
1.25 wt.% Nb	11.00	3.785	9.51
1.50 wt.% Nb	11.00	3.785	9.51
1.75 wt.% Nb	11.25	3.786	9.52

3.2 Photovoltaic Performance of DSSC. In order to determine the photovoltaic performance, the current density-voltage (J-V) curves of DSSC based on undoped and Nb-doped TiO_2 electrodes with different amounts of Nb dopant are shown in Fig. 2 and the photovoltaic properties are shown in Table 2. As shown in Table 2, the highest V_{OC} is found in the DSSC with 0.5-1.0 wt.% Nb-doped TiO_2. Higher V_{OC} value indicates the large energy difference between the conduction band of TiO_2 and the iodine redox potential. Due to the difference energy levels, the recombination of injected electron in the conduction band of TiO_2 with the oxidized electrolytes is prevented and resulting in higher efficiency for 1.0 wt.% Nb-doped TiO_2 [8].

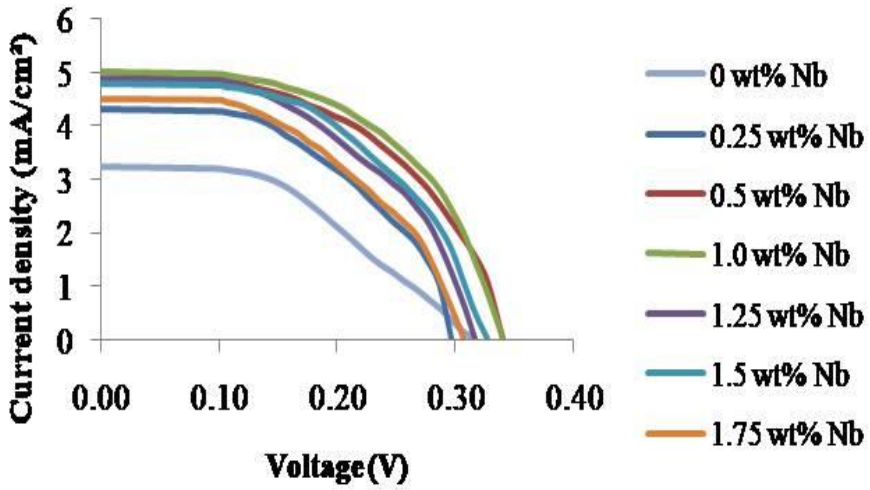

Fig. 2 The photocurrent density-photovoltage (J-V) of the fabricated DSSC using undoped and Nb doped TiO_2

Table 2 Photovolatic parameters of DSSC fabricated with undoped and Nb doped TiO_2

Sample	Jsc (mA/cm²)	V_{oc}/V	Efficiency, η (%)	Surface area (m^2/g)
0 wt.% Nb	3.20	0.32	0.80	6.1407
0.25 wt.% Nb	4.30	0.30	1.02	
0.5 wt.% Nb	5.00	0.33	1.32	
1.0 wt.% Nb	5.00	0.33	1.40	8.8314
1.25 wt.% Nb	4.90	0.32	1.27	
1.50 wt.% Nb	4.80	0.32	1.23	7.3451
1.75 wt.% Nb	4.50	0.30	1.08	

Improvement of V_{OC} also due to introduction of Nb into TiO_2 lattice improves the photo response due to additional energy levels was created within the band gap of TiO_2. The internal resistance decreases due to Nb dopants modified the electronic structure of TiO_2 therefore increase the V_{OC}. The highest J_{SC} of DSSC with 0.5-1.0 wt.% Nb-doped TiO_2 gave the highest value of 5.00 mA/cm². High J_{SC} values indicate high electron collection efficiencies which function as faster electron diffusion rates. The increase of J_{SC} and V_{OC} produced high efficiency which increases the performance of photovoltaic. Nb doping also reduces the concentration of

oxygen vacancies at the TiO_2 surface [10]. Therefore, the space charge region widened to suppress recombination at the TiO_2-electrolyte interface and leads to the increment of V_{OC} [11].The decrease in Voc and Jsc is also due to how Nb would have acted as a new recombination center thus reducing the number of charge carriers [12].

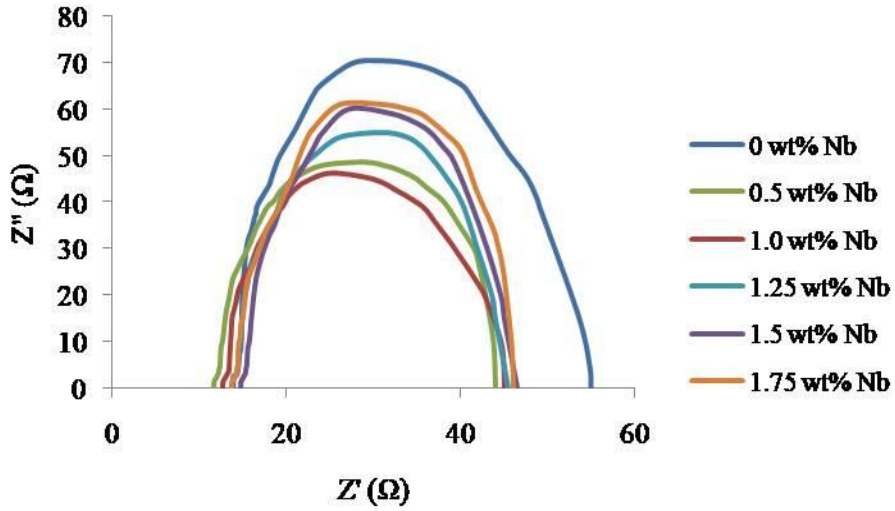

Fig. 3 Nyquist plots of DSSCs measured under illumination conditions for undoped and Nb-doped TiO_2

Electrochemical impedance spectroscopy (EIS) measurement was carried out to investigate the TiO_2/dye/electrolyte interfacial charge transfer kinetics. Fig. 3 shows the Nyquist plots for DSSC using undoped and Nb-doped TiO_2photoanodes. In Fig. 3, the charge transfer resistance related to the recombination of electrons (R_{CT}) at the photoanode/dye/electrolyte interface is determined using the semicircles at the intermediate frequency regions. The R_{CT} value for 1.0 wt.% Nb is the lowest compare to other dopants. It proves that electron transfer becomes faster within the TiO_2 film, implying that the film conductivity was improved [13]. Based on this result, it can be correlated that Nb dopant has improved the capacitance of the device leading to higher J_{SC} and V_{OC} values. However, when doping amount increases (1.25 wt.% Nb onwards), the R_{CT} increases due to the formation of more defects in the semiconductor. Higher R_{CT} value corresponds to lower probability in recombination of the electrons. The low recombination of electron leads the decreases of J_{SC} and V_{OC} values due to high recombination process.

4. SUMMARY

The performance of Nb-doped TiO_2 synthesized using the solid state method as photoanode promoted and favoured electron transformation. The DSSC with 1.0 wt.%Nb-doped TiO_2 improved the J_{SC} and V_{OC} and produced the highest efficiency of about 1.40%. The improvement of J_{SC} is related to the enhancement of electron injection and transportation. The reduction in the concentration of oxygen vacancies at the TiO_2 surface is correlated to Nb doping. Therefore, the space charge region was found to widen up and suppress electron recombination at the TiO_2-electrolyte interface and increase the value of Voc.

REFERENCES

[1] S. Zhang, X. Yang, Y. Numata, L. Han, Highly efficient dye-sensitized solar cells: progress and future challenges, Energy Environ. Sci., 6 (2013) 1443-1464.

[2] B. Tian, X. Zheng, T. J. Kempa, Coaxial silicon nanowires as solar cells and nanoelectronic power sources, Nature, 449 (2007) 885-889.

[3] S. Shakir, Z.S. Khan, A. Ali, Development of copper doped titania based photoanode and its

performance for dye sensitized solar cell applications, J. Alloy. Comp., 652 (2015) 331-340.

[4] P. Xiang, W. Ma, T. Xiao, L. Jiang, X. Tan, T. Shu, Ta-doped hierarchical TiO_2spheres for dye-sensitized solar cells, J. Alloy. Comp., 656 (2016) 45-50.

[5] C. Kim, K. Sim, H. Kim, Modification of a TiO_2photoanode by using Cr-doped TiO_2 with an influence on the photovoltaic efficiency of a dye-sensitized solar cell, J. Mater. Chem., 18 (2008) 5809-5814.

[6] X. Lü, X. Mou, J. Wu, D. Zhang, L. Zhang, F. Huang, F. Xu, S. Huang, Improved- performance dye-sensitized solar cells using Nb-doped TiO_2electrodes: efficient electron injection and transfer, Adv. Funct. Mater., 20 (2010) 509-515.

[7] T. Nikolay, L. Larina, O. Shevaleevskiy, B.T. Ahn, Electronic structure study of lightly Nb-doped TiO_2 electrode for dye-sensitized solar cells, Energy Environ. Sci., 4 (2011) 1480-1486.

[8] L. De Trizio, R. Buonsanti, A.M. Schimpf, A. Llordes, D.R. Gamelin, R. Simonutti, D.J. Milliron, Nb-doped colloidal TiO_2nanocrystals with tunable infrared absorption, Chem. Mater., 25 (2013) 3383-3390.

[9] J. Hidayani, Y. Madihan, Efficient dye-sensitized solar cells using *G. atroviridis*and *e. confertaf*ruits, Aust. J. Basic Appl. Sci., 37 (2015)367-370.

[10] H. Jaafar, Z.A. Ahmad, M.F. Ain, Effect of Nb-doped TiO_2photoanode using solid state method with *E. conferta* as sensitizer on the performance of dye sensitized solar cell,Optik., 144(2017) 91-101.

[11] S. Zhang, X. Yang, Y. Numata, L. Han, Highly efficient dye-sensitized solar cells:progress and future challenges, Energy Environ. Sci., 6 (2013) 1443-1464.

[12] L. Wei, X. Xia, Y. Yang, P. Wang, Y. Dong, T. Luan, Variable temperature spectroelectrochemistry study of silver-doped TiO_2 and its influence on the performance of dye sensitized solar cells, RSC Adv., 6 (2016) 68341-68350.

[13] H. Su, Y.T. Huang, Y.H. Chang, P. Zhai, N.Y. Hau, P.C.H. Cheung, W.T. Yeh, T.C. Wei, S.P. Feng,The synthesis of Nb-doped TiO_2nanoparticles for improved-performance dye sensitized solar cells, Electrochim. Acta, 182 (2015) 230-237.